Simulation Analysis of Electric Field of Air Gap Defect in 10KV XLPE Cable Based on COMSOL

Ziyan Zhu

Electric Power Engineering, Nanjing Institute of Technology, Nanjing, 211100, China

Keywords: Cross-linked polyethylene cable, Air gap, Finite element software, Electric field strength

Abstract: With the continuous advancement of urbanization and the improvement of people's living standards, power cables have become an important part of the power system; cross-linked polyethylene insulated cables have good electrical insulation properties, high mechanical strength, and high carrying capacity. The advantages have been widely used in high-pressure and ultra-high-pressure fields. However, during the manufacturing and operation of cables, small air bubbles may occur in the XLPE, which can cause distortion in the distribution of electric fields in the cable.The present study used the COMSOL finite element software for simulation to emulate the electric field in XLPE cables, specifically investigating the distribution features of bubbles of various sizes and locations in the 10kV XLPE cables. The results of the simulation show that the presence of bubbles inside the XLPE layer leads to a significant decrease in potential at the interface among the bubble with XLPE. Additionally, the electrical field intensity at the position of the bubble is greater compared to the electric field strength in the absence of bubbles.And as the position of the bubble gets closer to the outer layer of XLPE, the maximum field strength at the bubble becomes smaller.

1. Introduction

High-voltage cables can be divided into oil-impregnated paper insulated cables, plastic insulated cables, conductive adhesive insulated cables and rubber insulated cables according to different insulating media. The main materials used in the production process of high-voltage cables include polyvinyl chloride (PVC), cross-linked polyethylene (XLPE), thermoplastic elastomer (TPE), and silicone rubber[1]. However, cross-linked polyethylene insulated cables have advantages that other cables cannot match. It has a simple structure, light weight, no restrictions on laying, and has good thermomechanical properties, electrical properties and chemical corrosion resistance. It is one of the most widely used cables at present.During the production process of cables, if the mold is improperly selected or the materials used are wet when XLPE insulation is extruded, the factory cable insulation may contain certain bubbles, impurities, and moisture. During the prolonged operation of cable circuits, they can cause internal discharges within the insulation. Internal discharge is called partial discharge phenomenon. Partial discharge phenomenon that exists for a long time will increase the temperature of the cable, cause the insulation to form branches, accelerate the aging rate and even breakdown the insulation, causing the cable insulation to fail[2][3].Although the XLPE cable is highly

reliable, it is difficult to avoid tiny defects during the procedure of manufacturing, installation, operation and transportation. The defects of long-term electric-thermal effects gradually develop, which may eventually lead to the breakdown of the cable as shown in the figure as shown in the figure 1 shown[4].

Scholars at home and abroad have conducted a lot of research on the problem of air gap defects in cable joints. Hu Xinyu et al. [5]established a typical defect model of single-core XLPE cable joints to simulate the electric field and temperature field distribution of air gap defects, moisture defects and composite defects, and comparatively analyzed the diameter of air gap defects with different structural parameters and spatial positions. and axial electric field distribution characteristics. Deng Gaoyi et al. [6] established a 3D model of the cable intermediate joint. By setting typical single defects such as needle points and moisture, they introduced multiple composite defects during the on-site installation process, and used finite element analysis software to analyze the internal electric field distribution of the cable intermediate joint and compare. Wang Chunfeng et al. [7]conducted a study where they analyzed three common joint defect models of XLPE cables. They computed the cable's aging life under certain circumstances and compared it with the step-by-step withstand voltage experimental data. This allowed them to determine the life index of the chosen cable. Xia Junfeng et al. [8] established three typical defect geometric models: micropores inside the cable insulation, protrusions caused by the semiconducting shielding layer entering the insulation layer, and protrusions caused by the insulation entering the semiconducting shielding layer. The electric field at the defect was obtained through finite element analysis distribution, the effect of defect morphology on electric field distortion was studied.

This article uses 10kv cross -linked polyethylene high -voltage cables with different sizes and positions as a research object. It simulates the electric field by using the COMSOL finite element software[9]. To build a model in Comsol, you can clearly and intuitively see the distribution of the strong inner field of the XLPE layer; simultaneously, you can demonstrate the distribution and fluctuation pattern of robust distribution and change under various circumstances by generating a two-dimensional curve[10][11]. An analysis of the electric field's strength distribution in the XLPE cable under various situations provides a crucial benchmark for maintaining the cable's stability and assuring the dependability of power delivery.

Figure 1: Cable insulation breakdown photos

2. The creation of a cable prototype

2.1 Establishment of Simulation Model

The cross -linked polyethylene DC cable of the single core is generally squeezed by the five -layer structure of the copper guide core, the conductor shield, the XLPE insulating layer, the insulation shield, and the outer condom[12]. Construct a two-dimensional co-axis configuration of the cross-

linked polyethylene cable simulation model in Comsol to analyze the electric field intensity in the steady state inside the electrostatic field. Figure 2 displays the two-dimensional model. Table 1 displays the materials used in each layer and their corresponding relative dielectric constants. The calculation equation group of the electrostatic field is shown in the following formula (1) and (2).
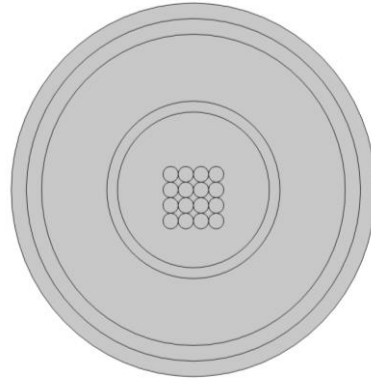
$$\nabla \bullet D = \rho_V \tag{1}$$

$$E = -\nabla V \tag{2}$$

Figure 2: XLPE cable structure schematic diagram

Table 1: Simulation material settings

Structure	Material	Relative permittivity
copper wire core	copper	0.0001
conductor shield	Silicone rubber	12
XLPE insulation layer	Ultra-smooth semiconducting cross-linked polyethylene	2.3
insulation shield	Silicone rubber	12
air gap	air	1
outer sheath	aluminum	0.0001

2.2 Creation of cable air gap fault model

During the cable extrusion process, due to the rough manufacturing process, Air gap faults often arise. The presence of air, moisture, and other significant contaminants inside the air gap will have an impact on the breakdown strength. Due to its weak polarity, XLPE has a relative dielectric constant. It is compact and has a high level of resistance to withstand voltage. Nevertheless, the interior structure of the air gap is intricate and the distribution of electric field strength is unequal. The collision-induced ionization of electrons and ions is likely to happen.When the ionization develops to a certain extent, breakdown is formed, thereby reducing the cable's strength. Insulating properties. Figure 3 and Figure 4 illustrates that the dimensions of bubbles often range from a few microns to several hundred microns. To enhance the visibility of the experimental data, various sizes of bubbles were included as independent variables in the experiment to detect the variations in electric field strength.
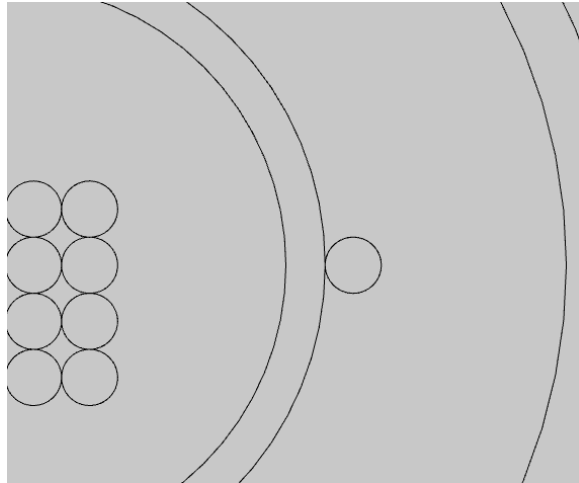
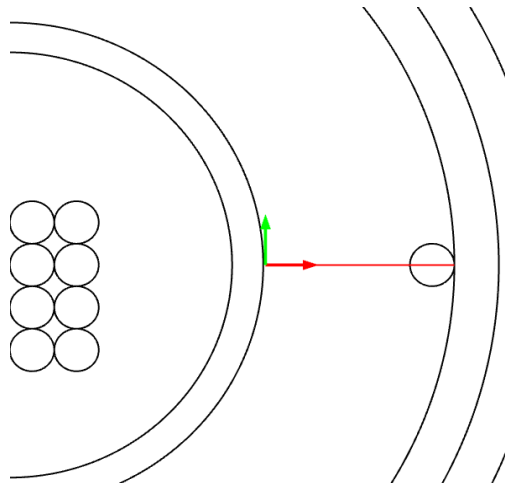Figure 3: Simulation model for air gap defects

Figure 4: Air gap defect two-dimensional section line graph

3. Results and analysis of the simulation

The finite element program COMSOL was used to obtain simulation results showing the distribution of electric field intensity for the XLPE cable without any flaws，as seen in Figure 5. From the results of Figure 5, it can be seen that the electric field inside the XLPE cable is large, the electric field intensity occurs at the contact among the wire core with the XLPE layer,has the highest value. From the defect-free radial electric field distribution curve in Figure 6, it can be seen that the electric field intensity near the conductor screen layer is the largest, and the electric field intensity away from the conductor shielding layer shows a decreasing trend, with a maximum value of around 3.1KV/mm.
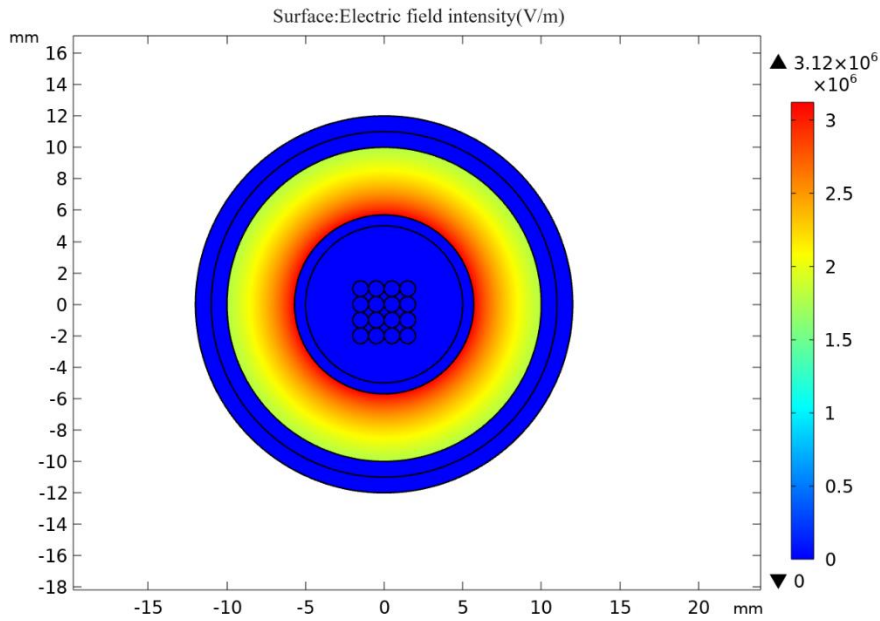
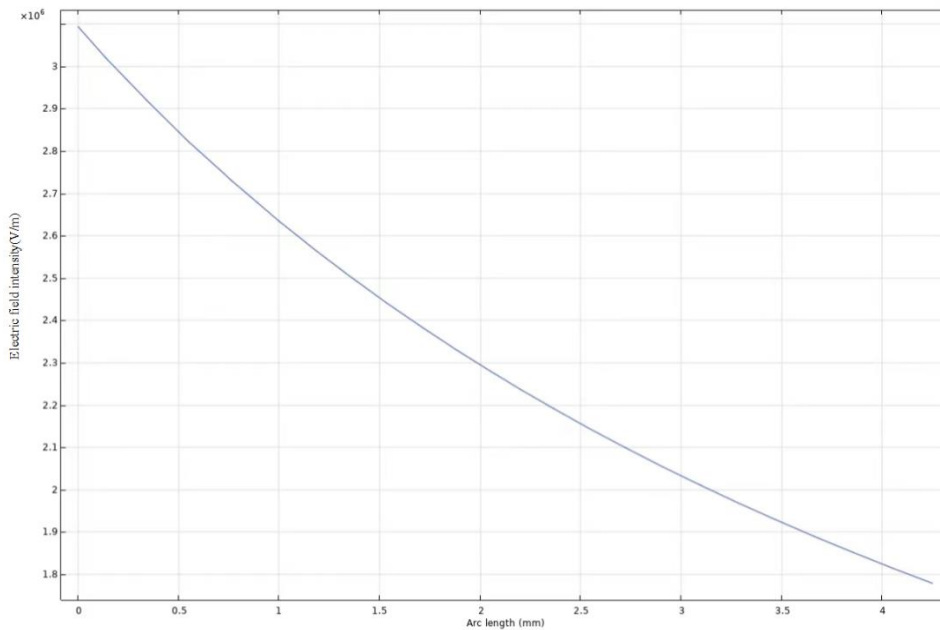Figure 5: Defect-free electric field distribution map

Figure 6: Radial electric field distribution curve without defects

3.1 Cables with air gaps in their internal structure have a significant impact on the intensity of the electric field inside them

Insert a circular small hole with a diameter of 1mm in the XLPE insulation layer to simulate the air gap defect. Figure 7 shows that there is obvious distortion at the strong field at the air gap. From the horizontal analysis, the potential near the air gap and the insulation layer's interchange decreased sharply, However, the power field strength at the electric field in the air gap is higher than the power field strength when the existence of the air gap. Observation from the radial upward, the maximum value of the field strength appears at the line core, and the strength of the electric field gradually decreases from the inside out from the inside out, and the near -ground side is 0. The distribution of

air gap defects along the radial electric field is shown in Figure 8. Because the relative dielectric constant at the air gap is less than the XLPE insulating layer, the power field strength at the connection of the two regions suddenly increases to 3.61kV/mm, an increase of approximately 16.5% compared with the maximum value of the maximum field.
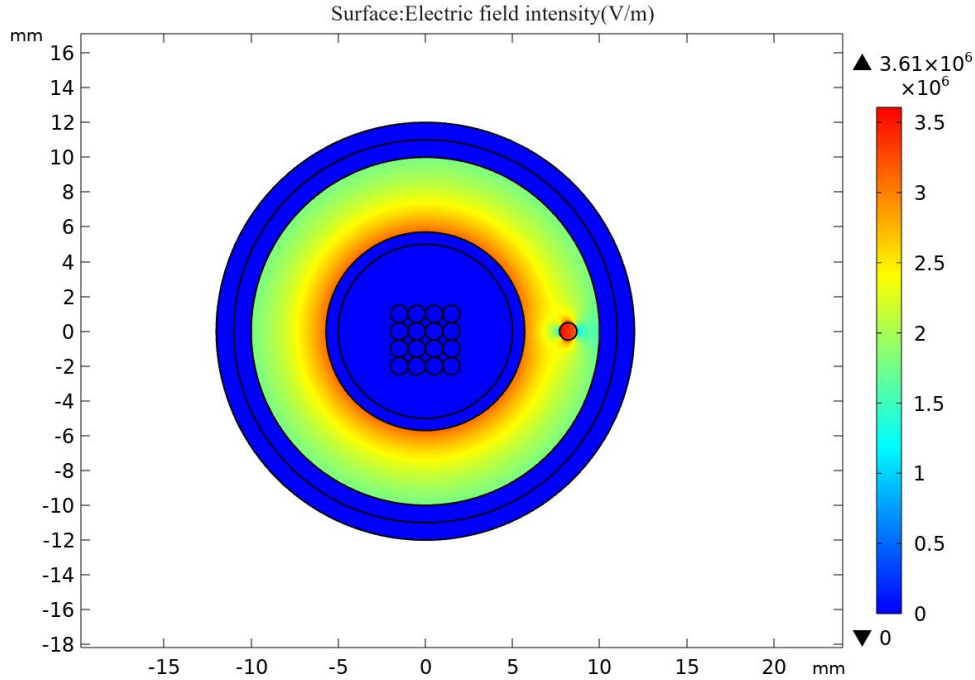
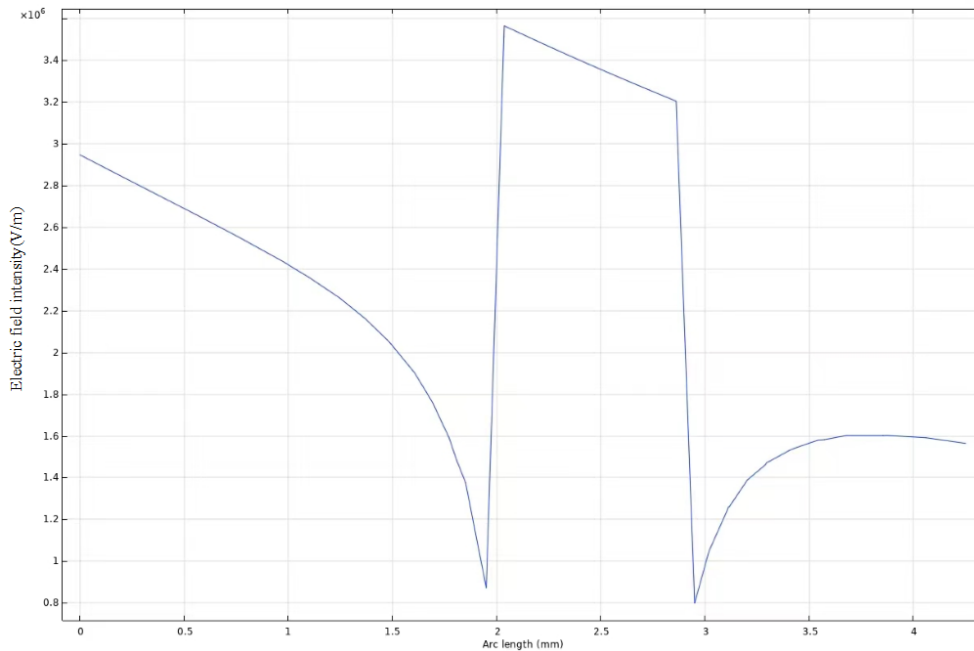

Figure 7: Bleuna defect distribution map

Figure 8: Air gap defect radial radial electric field distribution map

3.2 An analysis of the effects of changes in air gap on the strength of the field

Further analyzes the differences in the strength of the electric field when the size of the bubbles in XLPE changes. According to Figure 9, the bubble has a diameter of 0.5mm, which is smaller than

the defects above. The change in the strength of the electric field caused by smaller bubbles is small, and the threat to the safety operation of the cable is smaller. The specific value of the strength of the electric field is shown in Figure 10. It can be seen that as the diameter of the bubble decreases, the maximum strong value has decreased, and the range of field strong distortion is reduced.
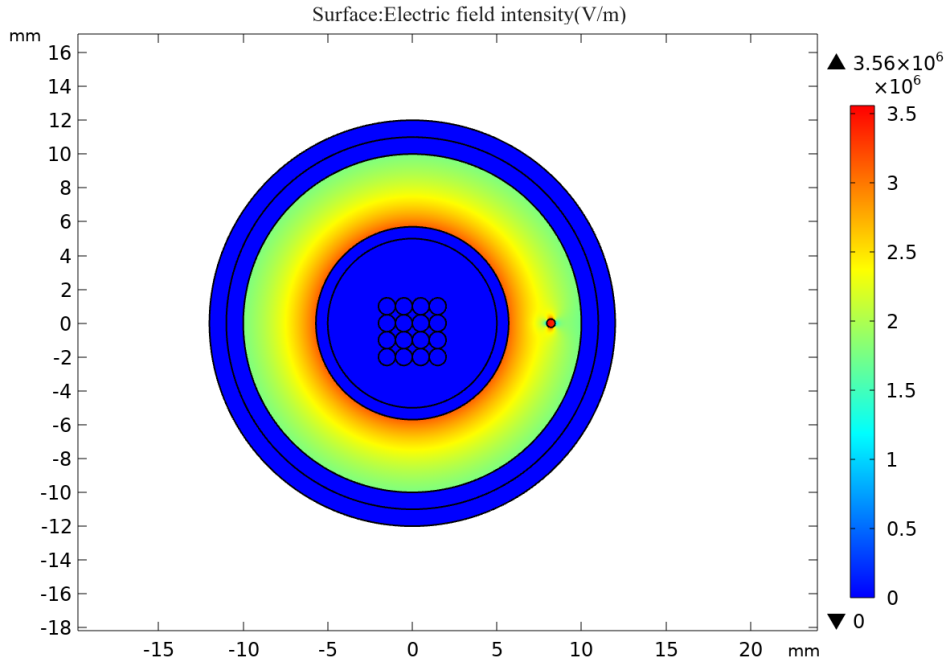

Figure 9: Field strong distribution map with bubble diameter is 0.5mm
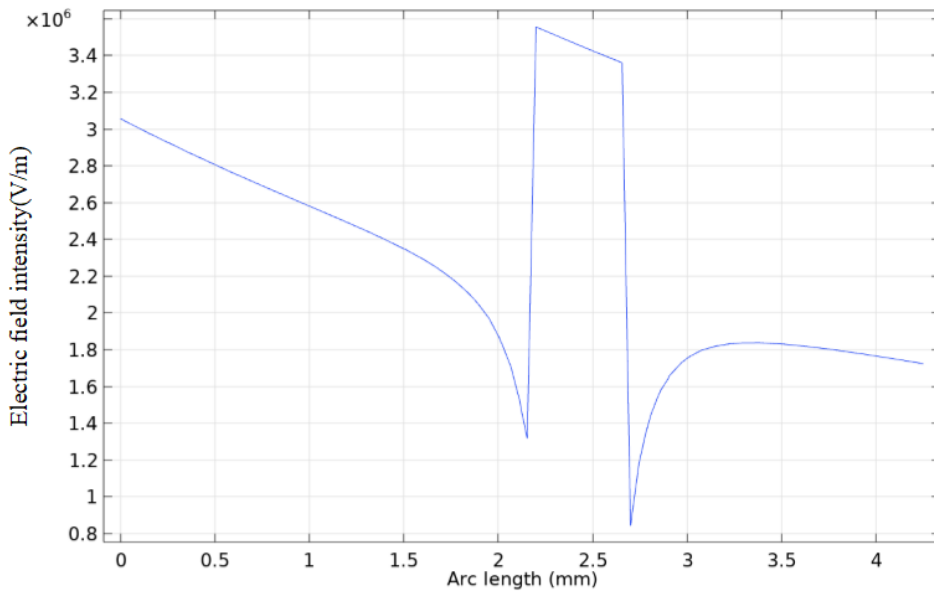

Figure 10: Radial electric field distribution curve of bubble diameter 0.5mm

When the location of the air gap defect stays constant, its magnitude is altered, resulting in the creation of a total of 6 air gap models. To enhance the clarity of the simulation findings, the air gap is positioned at a distance of 1mm from the conductor coating layer. Additionally, the diameters d1=0.125mm, d2=0.25mm, d3=0.5mm, d4=1mm, d5=1.5mm, and d6=2mm are used to evaluate the impact of various radial dimensions on the distribution of the electric field.

According to Figure 11, when the diameter is 0.125mm, the maximum field strength is

3.99KV/mm; when the diameter is 1mm, the maximum field strength increases to 4.1KV/mm; when the diameter is 2mm, the maximum field strength decreases to 3.86KV/mm. A widening air gap results in an increase in the strength of the electrical field, followed by a decrease.
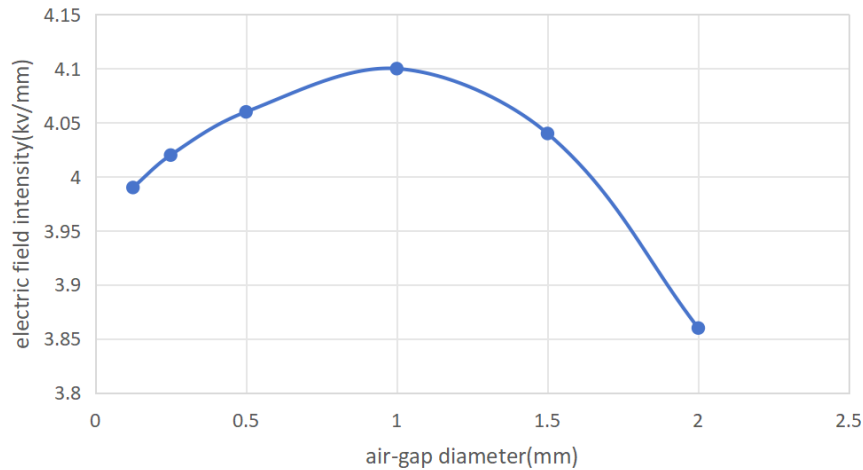

Figure 11: Electric field distribution curves of air gap defects with different radial

3.3 The impact of changes in the shape of the air gap on the field strength

In actual XLPE cables, irregular shape air shortage cables may appear. Different shapes of air gaps are different from the strength of the electric field strength. The oval cables are analyzed as an example. As shown in the Figure 12, the elliptical air gap is set in the same position. The long axis of the elliptical gap is 1mm and the short shaft is 0.5mm. The outcomes of the simulation are shown in Figure 13. It can be seen that the elliptical gap will also bring distortion field strength. The figure illustrates the specific value. This field has a maximum voltage of 3.2kV/mm.It can be seen that the degree of distortion of elliptical air gaps on the strength of the electric field is less.
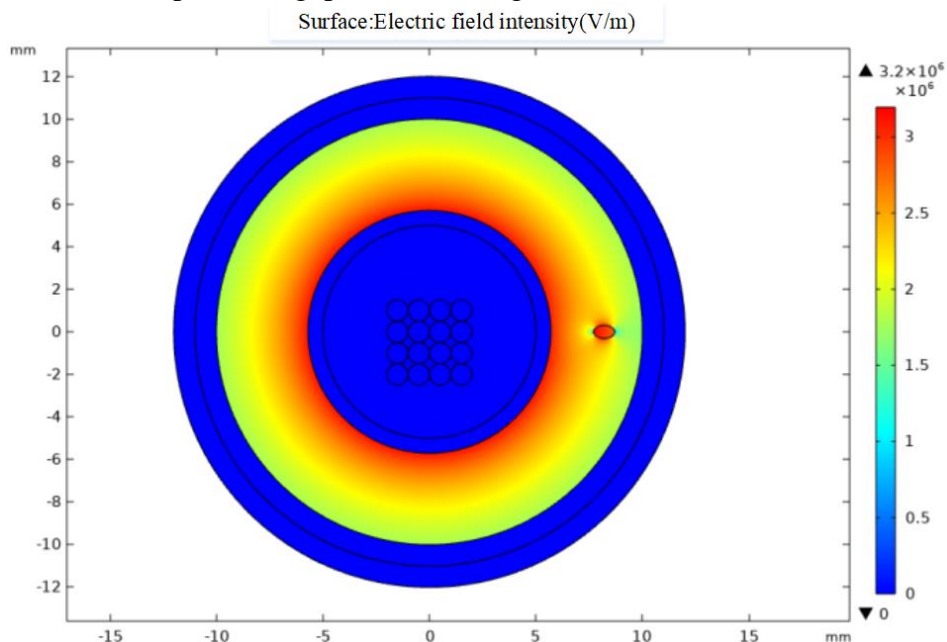

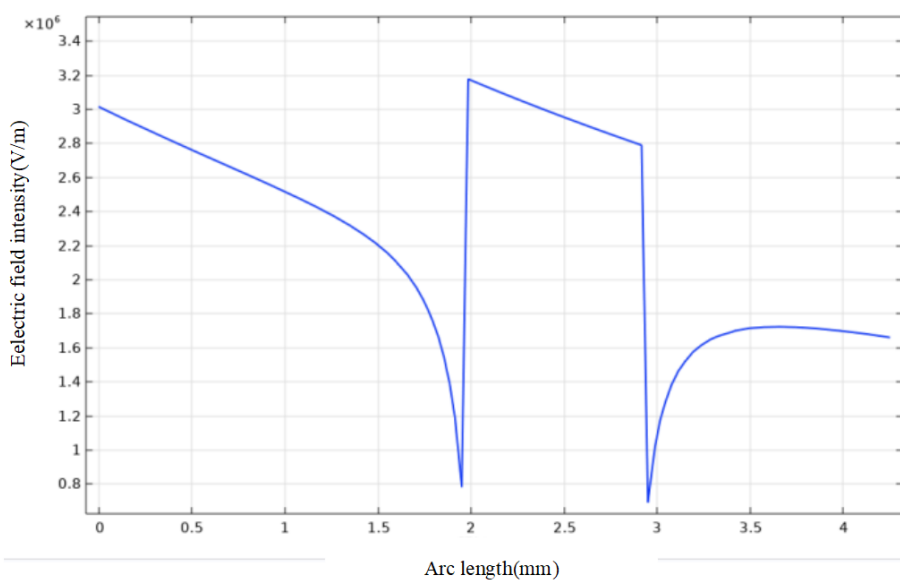Figure 12: Elliptical airfield distribution map

Figure 13: The radial electric field distribution curve of the oval gas gap

3.4 The impact of the distance between the internal gas gap defect in cable insulation and the conductor shielding layer on the electrical field strength

Keep the size of the air gap constant, change the distance from its to conductor shielding layer, and establish an entire set of six air gap defect models with a radius of 1mm. D4 = 2mm, D5 = 2.5mm, D6 = 3mm, and simulate the space position of the air gap with different values of distance. Starting from the surface of the conductor shielding layer, the outermost layer of the XLPE is the two - dimensional interception of the vertical passing through the air bubble heart. Figure 14 demonstrates that the electrical field strength is distorted at the air gap insulation. Additionally, the highest magnitude of field intensity value inside the air gap drops progressively as the distance rises. Simultaneously, when the distance between the air gap and the shielding layer increases, the maximum power field strength at the air gap likewise increases.
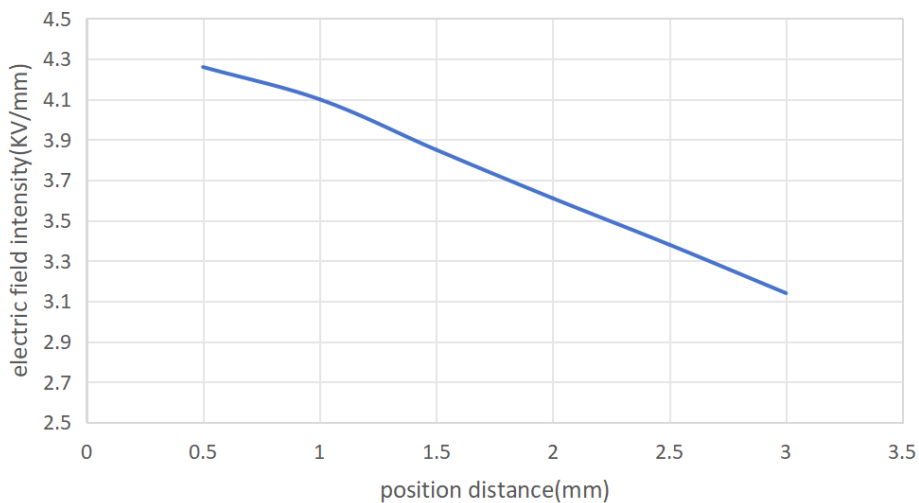

Figure 14: Electric field distribution curves of air gap defects at different locations

3.5 Effect of cable insulation layer thickness on electric field intensity distribution in the air gap

By keeping the location and size of the air gap defect constant, a total of 6 models were created by varying the thickness of the cable insulation layer[13]. Let's assume that the air gap has a diameter of 1 mm and is positioned precisely in the center of the insulating layer. The insulating layer is separated into several thicknesses to mimic the impact of varying insulation thicknesses on the dispersion of electric fields. The thicknesses are as follows: d1=5mm, d2=6mm, d3=7mm, d4=8mm, d5=9mm, and d6=10mm.

Figure 15 illustrates the results of the emulation. An insulating layer becomes thicker as the thickness of the insulating layer increases, resulting in a progressive decrease of the maximum field strength of the air gap, which is of the same size and position. As the insulation thickness increases, the maximum electric field strength decreases as the speed increases. It decelerates.
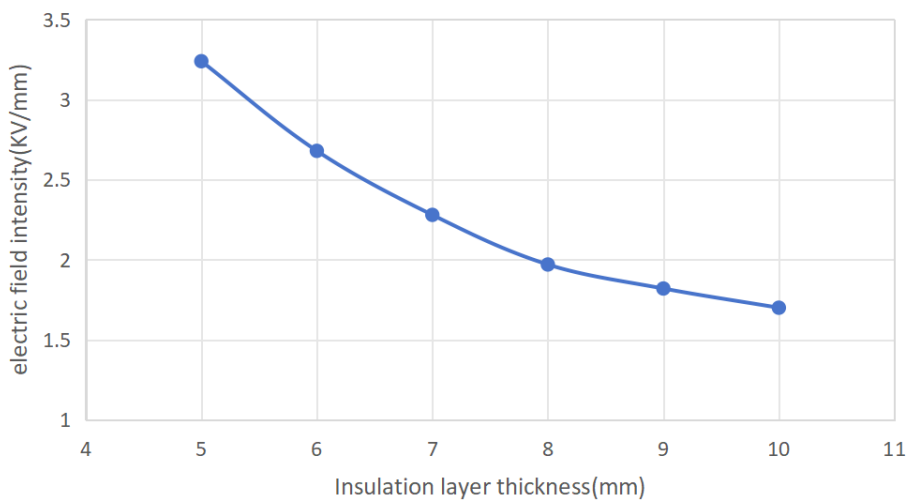

Figure 15: A graph showing how radial electric fields are distributed in a gap under different insulation thicknesses

4. Conclusion

To investigate the effects of bubble flaws in the XLPE layer of cross-linked polyethylene(XLPE) high-voltage cables on the electric field strength, this paper uses the COMSOL finite element software to conduct simulation experiments on bubble defects of different sizes and locations, and also observes and analyzes the corresponding Based on the distribution of electric field intensity, the relevant observations may be made:

(1) In the absence of any defects, the electric field intensity inside the XLPE cable decreases as the distance from the conductor shielding layer rises.

(2) When there is an air gap defect, the electric potential near the interface between the bubbles and the surrounding medium drops as the distortion weakens, leading to a reduction in the electric field intensity.

(3) The field intensity distribution of an air gap defect is determined by the size and location of the radius. The positional distance of an air gap of same size is inversely related to the maximum field strength. As the diameter of the air gap at the same distance grows, the electric field strength first rises and subsequently drops.

(4) There is a relationship between the thickness of the insulating layer and the distribution of field intensity that is affected by the presence of an air gap defect. When the size and position of the air gap are the same, the thickness of the insulating layer is inversely proportional to the maximum field

strength. The thickness of the insulating layer is inversely related to the maximum field strength when the size and location of the air gap remain constant.

References

[1] Ye Yongsheng, Deng Tengfei, Li Tuoneng, Liao Jinren. Overview of high-voltage cable materials and preparation processes for electric vehicles [J]. Automotive Parts, 2021, (01): 114-117.

[2] Hu Kai, Lu Zhifei, Yang Fengyuan, Zhang Lei, Zhang Yinxian. Research on typical defect simulation and partial discharge of high-voltage DC XLPE cable [C]. Zhejiang Electric Power Society 2018 Outstanding Papers Collection, 2018: 324-331.

[3] Du Hao, Guan Honglu, Chen Xiangrong, Hou Shuai, Yang Min, Wang Xin. Partial discharge characteristics of typical defects in cross-linked polyethylene cables under DC voltage [J]. High Voltage Technology, 2021, 47(02):555 -563.

[4] Su JG, Du BX, Li J, et al. Electrical tree degradation in high-voltage cable insulation: progress and challenges[J]. High Voltage, 2020, 5, (4):353-364.

[5] Hu Xinyu, Zhu Hui, Chen Xingang. Simulation study of electric field simulation of 10 KV XLPE cable joint defects [J]. Journal of Chongqing University of Science and Technology (Natural Science), 2022, 36(02): 171-178.

[6] Deng Gaoyi, Wang Xinghua, Nie Yixiong. Simulation study on electric field distribution of composite defects in the intermediate joint of 10 KV XLPE cable [J]. Wire and Cable, 2023, (05): 47-53.

[7] Wang Chunfeng, Sun Changhai, Li Duan, Hang Huifang, Chen Chen, Song Wenzhuo, Guo Furan. Aging life assessment of typical defects of cross-linked polyethylene cable joints [J]. Science, Technology and Engineering, 2020, 20(25): 10287- 10292.

[8] Xia Junfeng, Shi Nannan, Sun Jiansheng. Simulation analysis of the impact of typical defect shapes of high-voltage XLPE cable main insulation on electric field distortion [J]. Wire and Cable, 2022, (06): 1-6.

[9] Liu Peng, Wu Zehua, Zhu Sijia, Xu Jiazhong, Liu Qingdong, Peng Zongren. Simulation of the influence of defects on the electric field distribution of AC 1100kV GIL three-pillar insulator [J]. Journal of Electrical Engineering, 2022, 37(02): 469-478.

[10] Xuan Z , Shuting W , Ronghai L ,et al.Simulation of the Main Insulation Defects and Electric Field Numerical in 35 kV XLPE Cable Based on COMSOL[J].Yunnan Electric Power, 2015.

[11] Li Wenquan. High-voltage XLPE cable main insulation failure and faulty diagnosis and ranging study [J]. Electrical switch, 2021, 59 (01): 94-98.

[12] Liu Lingyu. Research on defect modeling and intelligent identification methods of urban underground transmission cable joints [D]. Shijiazhuang Railway University, 2023

[13] Yang Shuo, Geng Pulong, Qu Bingni, Song Jiancheng, Liu Jucai, Tian Min. Analysis of electric field distribution and influencing factors at air gap defects in mining high-voltage cable insulation [J]. Industrial and Mining Automation, 2018, 44(04):44-51